Neurological Sciences (2019) 40:779–791
https://doi.org/10.1007/s10072-019-3721-2

ORIGINAL ARTICLE

Protective effects of CX3CR1 on autoimmune inflammation in a chronic EAE model for MS through modulation of antigen-presenting cell-related molecular MHC-II and its regulators

Weihua Mai[1] · Xingwei Liu[2] · Junfeng Wang[1] · Jing Zheng[3] · Xiao Wang[2] · Wenying Zhou[4]

Received: 16 July 2018 / Accepted: 12 January 2019 / Published online: 23 January 2019

Abstract

Background Recent evidences have implicated neuroprotective effects of CX3CR1 in multiple sclerosis (MS). But whether CX3CR1 is involved in modulation of antigen-presenting cell (APC)–related molecular MHC-II and what the possible mechanism is remain unidentified.

Objective In this study, we intended to investigate the effects of CX3CR1 on MHC-II expressions on brain myeloid cells in experimental autoimmune encephalomyelitis (EAE) mice and explore the possible regulators for it.

Methods CX3CR1-deficient EAE mice were created. Disease severity, pathological damage, and the expressions of MHC-II and its mediators on myeloid cells were detected.

Results We found that compare with wile-typed EAE mice, CX3CR1-deficient EAE mice exhibited more severe disease severity. An accumulation of $CD45^{+}CD115^{+}Ly6C^{-}CD11c^{+}$ cells was reserved in the affected EAE brain of CX3CR1-deficient mice, consistent with disease severity and pathological damage in the brain. The expressions of MHC-II on the brain $CD45^{+}CD115^{+}Ly6C^{-}CD11c^{+}$ cells of CX3CR1-deficient EAE mice were elevated, in accord with the increased protein and mRNA expressions of class II transactivator (CIITA) and interferon regulatory factor-1 (IRF-1).

Conclusions The findings indicated that CX3CR1 might be an important regulator for MHC-II expressions on APCs, playing a beneficial role in EAE. The mechanism was probably through regulation on the MHC-II regulators CIITA and IRF-1.

Keywords Multiple sclerosis · Experimental autoimmune encephalomyelitis · CX3CR1 · Major histocompatibility complex class II molecules · Class II transactivator · Interferon regulatory factor-1

Introduction

Multiple sclerosis (MS) is a chronic, inflammatory demyelinating disease of the central nervous system (CNS), characterized by a relapsing-remitting or progressive disease course, causing irreversible neurological deficits in patients. It is considered as a predominantly T cell–mediated autoimmune disease, and experimental autoimmune encephalomyelitis (EAE) is its well-known animal model. Current treatments with immunomodulators are efficient in controlling the relapsing-remitting course, but fail to prevent disease progression. Therefore, to search for a reagent with neuroprotective effects is an urgent issue for future therapeutic strategies of MS.

CX3CL1 (fractalkine) is a distinct chemokine, constitutively expressed by neurons in the CNS, while its specific unique receptor, CX3CR1, is exclusively expressed by microglia [1–4]. Except for promoting tissue inflammation via recruitment of immune cells to these sites, recent studies have identified a

Weihua Mai and Xingwei Liu contributed equally to this work and should be considered co-first author

✉ Weihua Mai
weihuamai2004@163.com

[1] Department of Neurology, The Fifth Affiliated Hospital of Sun Yat-sen University, NO. 52 East Meihua Road, Zhuhai 519000, Guangdong Province, China

[2] Department of General Surgery, The Fifth Affiliated Hospital of Sun Yat-sen University, Zhuhai, China

[3] Department of Nephrology, The Fifth Affiliated Hospital of Sun Yat-sen University, Zhuhai, China

[4] Department of Laboratory Science, The Fifth Affiliated Hospital of Sun Yat-sen University, Zhuhai, China

protective role of CX3CL1-CX3CR1 in certain pathological conditions. It was shown that variant alleles of CX3CR1 (I249 and M280) could result in decreased CX3CL1-binding affinity and lower expression of CX3CR1, contributing to the development of age-related macular degeneration [5, 6]. In addition, in three pathological models including Parkinson's disease, amyotrophic lateral sclerosis, and endotoxemia, CX3CR1-deficient mice exhibited more extensive neuronal loss and microglial neurotoxicity, indicating a neuroprotective role of CX3CR1 in the CNS [3]. The neuroprotective role of CX3CL1-CX3CR1 was also reported in hippocampal neurons, mediated through the adenosine receptor 1 [7–9].

Recent evidence also implicated neuroprotective effects of CX3CL1-CX3CR1 in MS. It was shown that CX3CR1-deficient EAE mice exhibited more severe neurological deficits, correlated with enhanced brain inflammation, demyelination, and neuronal damage [10]. A genetic study revealed a lower frequency of $CX3CR1^{I249/T280}$ haplotype in patients with secondary progressive MS (SPMS) compared with relapsing-remitting MS, indicating that $CX3CR1^{I249/T280}$ haplotype could have protective effect for switch to SPMS [11]. But as to the mechanism for the neuroprotective role of CX3CR1 in MS, less was known. Reduced recruitment of NK cells in $CX3CR1^{GFP/GFP}$ mice with EAE was visualized, which was associated with increased disease severity [12]. Enrichment of $CD115^{+}Ly6C^{-}CD11c^{+}$ dendritic cells was also observed in the affected EAE brain of CX3CR1-deficient mice, where this particular cell subset might be involved in anti-myelin T cell stimulation, implicating an important role of CX3CR1 for antigen-presenting cells (APCs) in MS [10].

However, whether CX3CR1 is involved in the function of APCs (modulation of antigen presentation) and what the possible mechanism is remain unidentified. Major histocompatibility complex class II molecules (MHC-II), a set of surface proteins on APCs, are known to be essential for the primary recognition during T cell activation. The regulation of MHC-II gene expression is complicated, involving several transcriptional factors acting on the MHC-II promoters. Class II transactivator (CIITA) is the master MHC-II gene regulator, while signal transducers and activators of transcription (STAT) molecules and interferon regulatory factor-1 (IRF-1) also participate in the regulation of MHC-II expression [13].

In the current study, we intended to investigate the alternation of MHC-II expression on myeloid cells in the brain of CX3CR1-deficient EAE mice and explore the possible mechanism for it. We supposed that the expressions of MHC-II on $CD115^{+}Ly6C^{-}CD11c^{+}$ dendritic cells in the affected EAE brain of CX3CR1-deficient mice were elevated, which correlated with neurological deficits and brain pathology. The expressions of CIITA and IRF-1 in the affected brain of CX3CR1-deficient EAE mice were also increased, possibly involved in the mechanism linking CX3CR1 and modulation of MHC-II expression on APCs. CX3CR1 might be an important regulator for APC function, playing a neuroprotective role in a chronic EAE model for MS.

Material and methods

Generation of CX3CR1-deficient mice

Wild-type C57BL/6 mice were obtained from the Animal Experiment Center of Sun Yat-sen University. CX3CR1-deficient mice were generated according to the methods described by Jung S before [14]. Briefly, the mutant murine CX3CR1 locus was constructed by targeted replacement of the CX3CR1 gene (the first 390 bp of the second CX3CR1 coding exon) with the cDNA encoding EGFP (pEGFP-N1; GenBank accession no. U55762; bp 653 to 1666; Clontech). Following homologous recombination and after neo gene deletion, the isolated targeted embryonic stem cell clones (E14.1, 129/Ola) were injected into blastocysts to generate chimeric mice. Germ line transmission of the mutant allele yielded heterozygous mutant $CX3CR1^{+/GFP}$ mice, which were intercrossed to generate $CX3CR1^{GFP/GFP}$ mice. Mice were genotyped by RT-PCR using cDNA reverse-transcribed from lymphoid tissues and the chemokine receptor-specific primers listed in Table 1. All animal experimental procedures were performed in accordance with the Guidelines of Animal Care approved by the Local Ethical Committee at the Fifth Affiliated Hospital of Sun Yat-sen University.

EAE induction

To induce EAE, 6–8-week-old CX3CR1-deficient ($CX3CR1^{GFP/GFP}$) and wild-type (WT) female mice were immunized subcutaneously with 100 μg myelin oligodendrocyte glycoprotein ($MOG_{35–55}$, orb72986, Biorbyt, San Francisco, CA, USA) peptide emulsified 1:1 in complete Freund's adjuvant (CFA, KX0210046-10, Beijing Biodragon Immunotechnologies Company, Beijing, China) containing 5 mg/ml heat-inactivated mycobacterium tuberculosis. Two hundred nanograms of pertussis toxin (1045840, Xiya Reagent, Shandong, China) was injected intraperitoneally on the day of immunization and repeated 48 h later. Mice were weighted and monitored daily, scored as below: 0 = healthy; 1 = limp tail; 2 = ataxia and/or paresis of the hindlimbs; 3 = paralysis of the hindlimbs and/or paresis of the forelimbs; 4 = tetraparalysis; 5 = moribund or death [15]. Mice were sacrificed at the peak of EAE disease (16–21 days postimmunization).

Flow cytometry

$CX3CR1^{GFP/GFP}$ and WT EAE mice at the peak of EAE were transcardially perfused with PBS. Brain tissues were dissected, followed by digestion with enzymatic digestion kit

Table 1 PCR primer-specific for wild and mutant CX3CR1 alleles

Gene	Primer[a]	Primer sequences	Amplified fragment size (bp)
Wild CX3CR1 allele	Forward (A) Reverse (B)	5′-CCTTTGCCGGGGAAAAGTTC-3′ 5′-TTTGTCACCAGTAAGCCCCA-3′	394
Mutant CX3CR1^{GFP} allele	Forward (C) Reverse (B)	5′-ATCATGGCCGACAAGCAGAA-3′ 5′-TTTGTCACCAGTAAGCCCCA-3′	744

[a] Primer A hybridized to the first 388 bp of the second CX3CR1 coding exon. Primer B hybridized to the upstream untranslated exon of CX3CR1. Primer C hybridized to the EGFP gene

(KGA829, KeyGenBioTech, Nanjing, China) according to the manufacturer's instructions. After passing through a 70-μm nylon mesh and wash, single-cell suspensions were prepared. Then, cells were incubated on ice for 15~20 min with a mix of fluorochrome-conjugated anti-mouse antibodies: CD45-PE-Cyanine7 (30-F11, eBioscience, San Diego, CA, USA), CD115-APC (AFS98, eBioscience, San Diego, CA, USA), CD11c-PE (N418, eBioscience, San Diego, CA, USA), Ly6C-eFluor 450 (HK1.4, eBioscience, San Diego, CA, USA), and MHC-II (I-Ab)-FITC (AF6-120.1, eBioscience, San Diego, CA, USA) using single-stained samples as controls. After wash, cells were resuspended in PBS. The respective antigens of the used antibodies were CD45, CD115, CD11c, Ly6C, and MHC-II. And the events used in each FACS assay were 1.8×10^6. Fluorescence profiles were acquired on Gallios flow cytometer (Beckman Coulter, Kraemer Boulevard Brea, CA, USA) and the data were analyzed with FlowJo 7.6 Analysis software.

Immunohistochemistry

Brains and spinal cords of CX3CR1$^{GFP/GFP}$ and WT EAE mice, as well as CX3CR1$^{GFP/GFP}$ and WT naive mice, were dissected, post-fixed in 4% paraformaldehyde, then processed for paraffin embedding and tissue section (4~6 μl) cutting. After inactivation of endogenous peroxidases and blockage of nonspecific binding, the sections were incubated overnight at 4 °C with rabbit anti-CD45 pAbs at 1:1000 (ab10558, Abcam, Cambridge, MA, USA), mouse anti-myelin basic protein mAbs (MBP101) at 1:1000 (ab62631, Abcam, Cambridge, MA, USA), or rabbit anti-calbindin pAbs at 1:1000 (ab11426, Abcam, Cambridge, MA, USA). Then, the sections were incubated with biotin-conjugated goat anti-rabbit or goat anti-mouse immunoglobulins at 1:100 (IB-0061/IB-0021, Beijing DingguoChangsheng Biotechnology, Beijing, China), followed by incubation with horseradish peroxidase (HRP)–labeled streptavidin at 1:200 (IH-0061, Beijing DingguoChangsheng Biotechnology, Beijing, China) at 37 °C for 40 min. The action cascade was visualized by incubation with diaminobenzidine (DAB) as a substrate, followed by counterstain with Nissl. For Nissl staining, after tissues were mounted onto sides, sections were de-fat on gradient ethanol (100%, 95%, and 70%) then stained in 0.5% cresyl violet for 3 min, followed by dehydration in graded ethanol (70%, 95%, and 100%). Then, slides were cleared in xylene for 5 min twice and mounted with permanent mounting medium. Three tissue sections per mouse ($n = 2$ per group) were imaged. The integrated optical density (IOD) of myelin immunoreactivity in each image was measured using Image-Pro Plus 6.0 (Media Cybernetics, Inc. Rockville, MD, USA).

Western blotting

After lysed by radioimmunoprecipitation assay (RIPA) lysis buffer plus phenylmethyl sulfonyl fluoride (PMSF), the protein concentrations of brain cells were assessed using a

Table 2 PCR primer sequences for MHC-II, CIITA, IRF-1, CX3CR1 and GAPDH

Gene	Primer	Primer sequences	Amplified fragment size (bp)
MHC-II	Forward Reverse	5′-CAAGGACTGAGGGCGGAAAC-3′ 5′-CCCACTCCTCCCGGTTGTAG-3′	126
CIITA	Forward Reverse	5′-TCACCTTCACGGTCACTACA CT-3′ 5′-CAGCCTGACTTCTGGGTTGG-3′	266
CX3CR1	Forward Reverse	5′-TACACAAGCGAGGGAGATGG-3′ 5′-ACCAGTAAGCCCCAATGTTCA-3′	242
IRF-1	Forward Reverse	5′-AAAGGGACATAACTCCAGCAC-3′ 5′-GCTTCATAAGGTCTTCGGCTA-3′	192
GAPDH	Forward Reverse	5′-AGGTCGGTGTGAACGGATTTG-3′ 5′-GGGGTCGTTGATGGCAACA-3′	95

bicinchoninic acid (BCA)-100 Protein Quantitative Analysis Kit (BCA01, Beijing DingguoChangsheng Biotechnology, Beijing, China), on a Model 550 microplate reader. Protein samples were electrophoresed by SDS-PAGE (sodium dodecyl sulfate polyacrylamide gel electrophoresis) and transferred to polyvinylidene difluoride (PVDF) membrane (Pall Life Sciences, New York City, NY, USA) at 110 mA for 2~3 h. After blocked in 5% skimmed milk in TBST (Tris-buffered saline-Tween 20) for 1 h, the blots were incubated with the following primary antibodies overnight at 4 °C: rabbit anti-CX3CR1 at 1:500 (ab217291, Abcam, Cambridge, MA, USA), rabbit anti-MHC-II at 1:1000 (ab180779, Abcam, Cambridge, MA, USA), rabbit anti-CIITA at 1:1000 (ab49132, Abcam, Cambridge, MA, USA), and rabbit anti-IRF-1 (EPR18301) at 1:1000 (ab186384, Abcam, Cambridge, MA, USA) using rabbit anti-β-actin at 1:5000 (ab179467, Abcam, Cambridge, MA, USA) as loading control. Then, the blots were incubated with HRP (horseradish peroxidase)-conjugated goat anti-rabbit antibodies at 1:5000 (BA1054, Wuhan Boster Biological Technology, Wuhan, China) for 1 h. Immunoreactivity of primary antibodies was detected using an enhanced chemiluminescence (ECL) detection kit (Pierce, Thermo Scientific, Waltham, MA, USA), and images were acquired using a Kodak film (Kodak, Rochester, NY, USA). The protein bands were analyzed using Image J software.

Quantitative real-time reverse transcription polymerase chain reaction

Total RNA was extracted from the cerebral tissues dissected from wild-type and CX3CR1$^{GFP/GFP}$ EAE mice at the peak of EAE, using TRIzol reagent (10296010, Invitrogen, Waltham, MA, USA) according to the manufacturer's instructions. The concentration and purity of RNA were assessed by ultraviolet spectrophotometer Q5000 (Quawell Technology Inc., Sunnyvale, CA, USA), and the RNA integrity was evaluated in 1% agarose gels. RNA was reverse-transcribed to complementary DNA (cDNA) by employing moloney murine leukemia virus reverse transcriptase (M-MLV RT, 28025013, Invitrogen, Waltham, MA, USA), using an oligo dT primer. Quantitative real-time PCR was performed using Fast SYBR Green Master Mix Bulk Pack (4385612, Invitrogen, Waltham, MA, USA) with 2 μl of cDNA template in a 20-μl reaction, analyzed on ABI PRISM 7500 Sequence Detection System (Applied Biosystems, Waltham, MA, USA). The relative quantitation value was calculated with the $2^{-\Delta\Delta Ct}$ method, using GAPDH as an internal control. The primer sequences for MHC-II, CIITA, IRF-1, CX3CR1, and GAPDH were listed in Table 2.

Statistical analysis

Comparisons among groups were analyzed using one-way analysis of variance (ANOVA) and non-parametric Mann-Whitney *U* test as appropriate. Pairwise comparisons were tested by least significant difference (LSD). Pearson's correlation coefficients were used for correlation analysis. Data were shown as mean ± SEM (standard error of mean). All statistical procedures were performed using the statistical package of the social sciences 19.0 (SPSS 19.0). $P < 0.05$ was considered to be significant.

Results

Genotype of CX3CR1-deficient mice

WT, CX3CR1$^{+/GFP}$, and CX3CR1$^{GFP/GFP}$ mice were genotyped by PCR using DNA extracted from lymphoid tissues. It was shown that in CX3CR1$^{+/GFP}$ mice, two DNA fragments (394 bp and 744 bp) were observed, indicating that both WT and mutant CX3CR1 transcripts were presented. In CX3CR1$^{GFP/GFP}$ mice, only mutant CX3CR1 transcripts (744 bp) were visualized, but WT CX3CR1 transcripts (394 bp) were absent (Fig. 1).

Increased disease severity in CX3CR1-deficient EAE mice

CX3CR1$^{GFP/GFP}$ and WT mice were immunized with $MOG_{35–55}$ peptide and monitored daily. Compared with WT mice, CX3CR1$^{GFP/GFP}$ mice developed EAE with earlier onset (13.36 ± 0.509 vs 17.00 ± 0.756 days, $P = 0.000$, $F = 15.972$) and reached the peak of disease earlier (17.93 ± 0.808 vs 20.64 ± 0.746 days, $P = 0.020$, $F = 6.091$). The maximum EAE scores were also higher in CX3CR1$^{GFP/GFP}$ mice (3.00 ± 0.166 vs 2.18 ± 0.135, $P = 0.001$, $F = 14.789$). The results were presented in Fig. 2.

Enrichment of CD45$^+$CD115$^+$Ly6C$^-$CD11c$^+$ dendritic cells in the brain correlated with enhanced CNS pathology in CX3CR1-deficient EAE mice

Brain cells isolated from CX3CR1$^{GFP/GFP}$ and WT EAE mice at peak of disease were analyzed by flow cytometry using antibodies against CD45, CD115, CD11c, and Ly6C. CD45$^+$-infiltrating leucocytes were gated for further analysis on CD115, CD11c, and Ly6C expressions to distinguish different myeloid cell subsets. As a result, it was shown that compare with WT EAE mice, the proportion of CD45$^+$CD115$^+$Ly6C$^-$CD11c$^+$ cells was dramatically increased in CX3CR1$^{GFP/GFP}$ EAE mice ($63.6 \pm 2.12\%$ vs $17.6 \pm 0.74\%$, $P = 0.000$, $F = 420.34$), indicating that CD45$^+$CD115$^+$Ly6C$^-$CD11c$^+$ cells were the major infiltrating myeloid cell population in CX3CR1$^{GFP/GFP}$ EAE mice.

To investigate the relationship of infiltrating myeloid cells and CNS pathology in WT and CX3CR1$^{GFP/GFP}$ EAE mice,

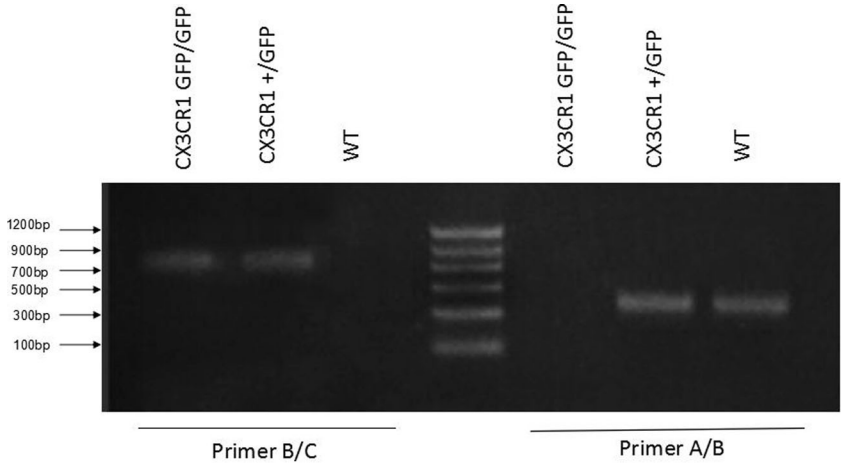

Fig. 1 Genotype of wild-type, CX3CR1$^{+/GFP}$, and CX3CR1$^{GFP/GFP}$ mice. Wild-type (WT), CX3CR1$^{+/GFP}$, and CX3CR1$^{GFP/GFP}$ mice were genotyped by RT-PCR using cDNA reverse-transcribed from lymphoid tissues and the chemokine receptor-specific primers. Primer A hybridizing to the first 388 bp of the second CX3CR1 coding exon was combined with primer B hybridizing to the upstream untranslated exon of CX3CR1, to amplify a 394-bp fragment indicative of the WT CX3CR1 allele. The combination of primer B with primer C hybridized to the EGFP gene, produced a 744-bp fragment indicative of the mutant CX3CR1^{GFP} allele

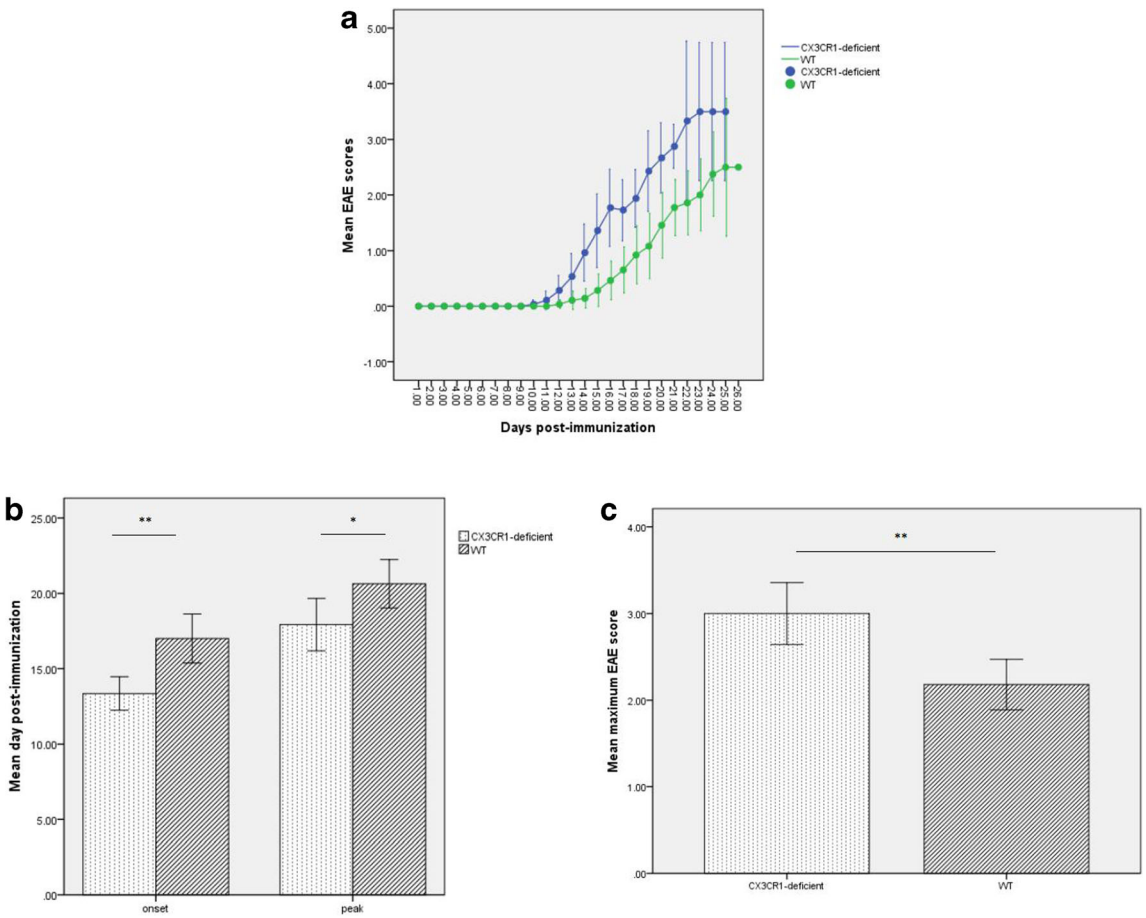

Fig. 2 Comparison of disease onset and EAE scores between wild-type (WT) and CX3CR1-deficient EAE mice. **a** WT ($n = 14$) and CX3CR1$^{GFP/GFP}$ mice ($n = 14$) were immunized with $MOG_{35–55}$ peptide and monitored daily. EAE scores were recorded. **b** Compared with WT mice, CX3CR1$^{GFP/GFP}$ mice developed EAE with earlier onset and reached the peak of disease earlier. **c** The maximum EAE scores were also higher in CX3CR1$^{GFP/GFP}$ mice. Data were presented as mean ± SEM. $^{*}P < 0.05$, $^{**}P < 0.01$ by one-way ANOVA (versus WT EAE mice)

brains and spinal cords were sectioned and analyzed by IHC at the peak of disease, using CD45, MBP, and calbindin as a marker of inflammation, demyelination, and Purkinje cells, respectively. As presented in Fig. 3A and B, compared with WT naive and CX3CR1$^{GFP/GFP}$ naive mice, CD45^{+} inflammatory cells were evident in the brains and spinal cords of WT and CX3CR1$^{GFP/GFP}$ EAE mice, but more prominent in CX3CR1$^{GFP/GFP}$ EAE mice, indicating that inflammatory infiltrates were more severe in CX3CR1$^{GFP/GFP}$ EAE mice. It was also observed that myelin staining (MBP-positive areas)

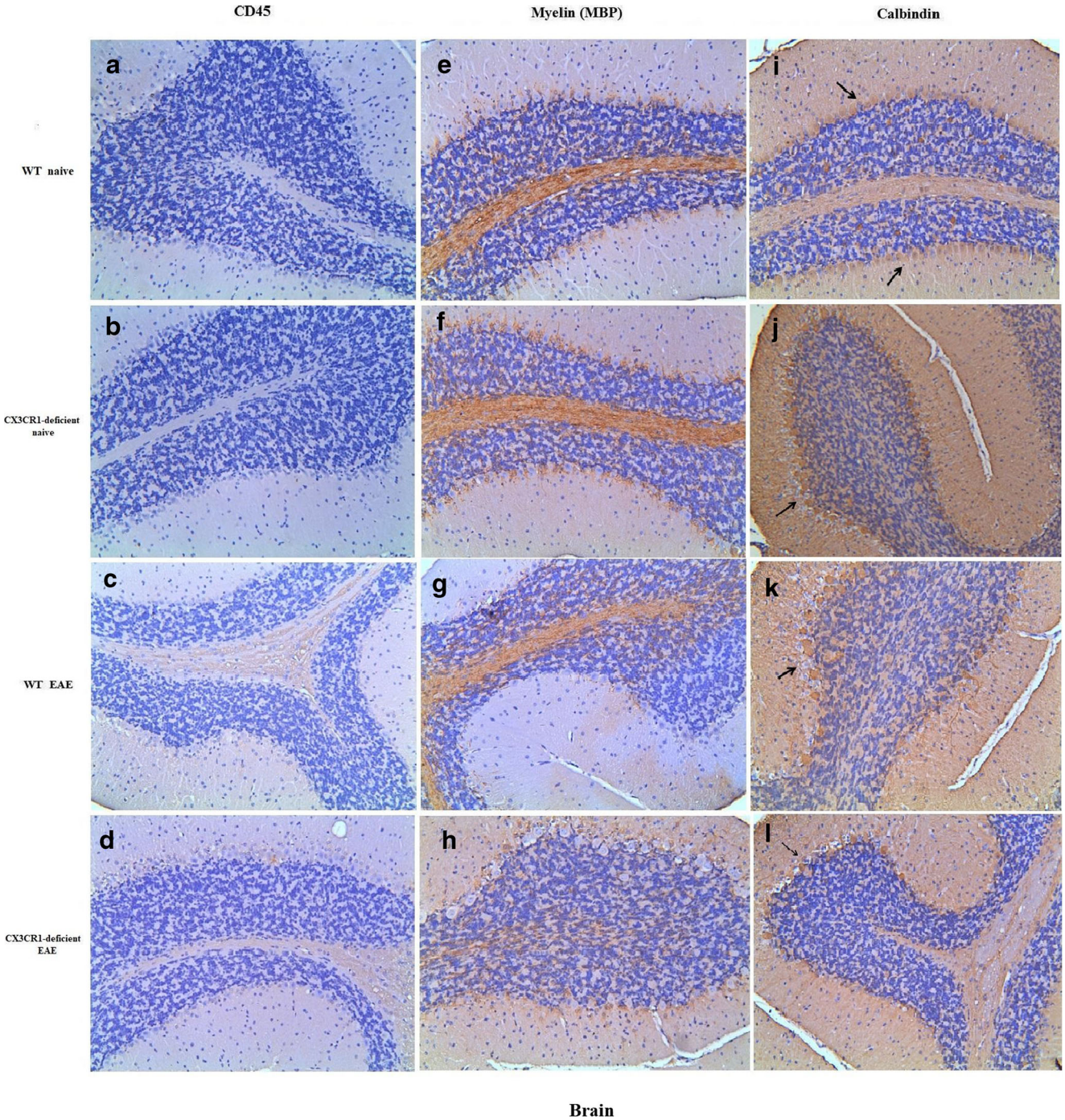

Fig. 3 More severe CNS pathology in CX3CR1-deficient EAE mice. Brains and spinal cords were sectioned and analyzed by IHC, using anti-CD45, anti-MBP, and anti-calbindin antibodies to detect inflammation, demyelination, and Purkinje cell damage, respectively. Compared with CX3CR1-deficient naive, wild-type (WT) naive, and WT EAE mice, CD45^{+} infiltrating leucocytes were more prominent in CX3CR1-deficient EAE mice (A, a–d and B, m–p). The intensity of the myelin staining decreased more dramatically (A, e–h and B, q–t), and calbindin-positive neurons were destroyed with the disruption of the granular cell layer in CX3CR1-deficient EAE mice (A, i–l and B, u–x)

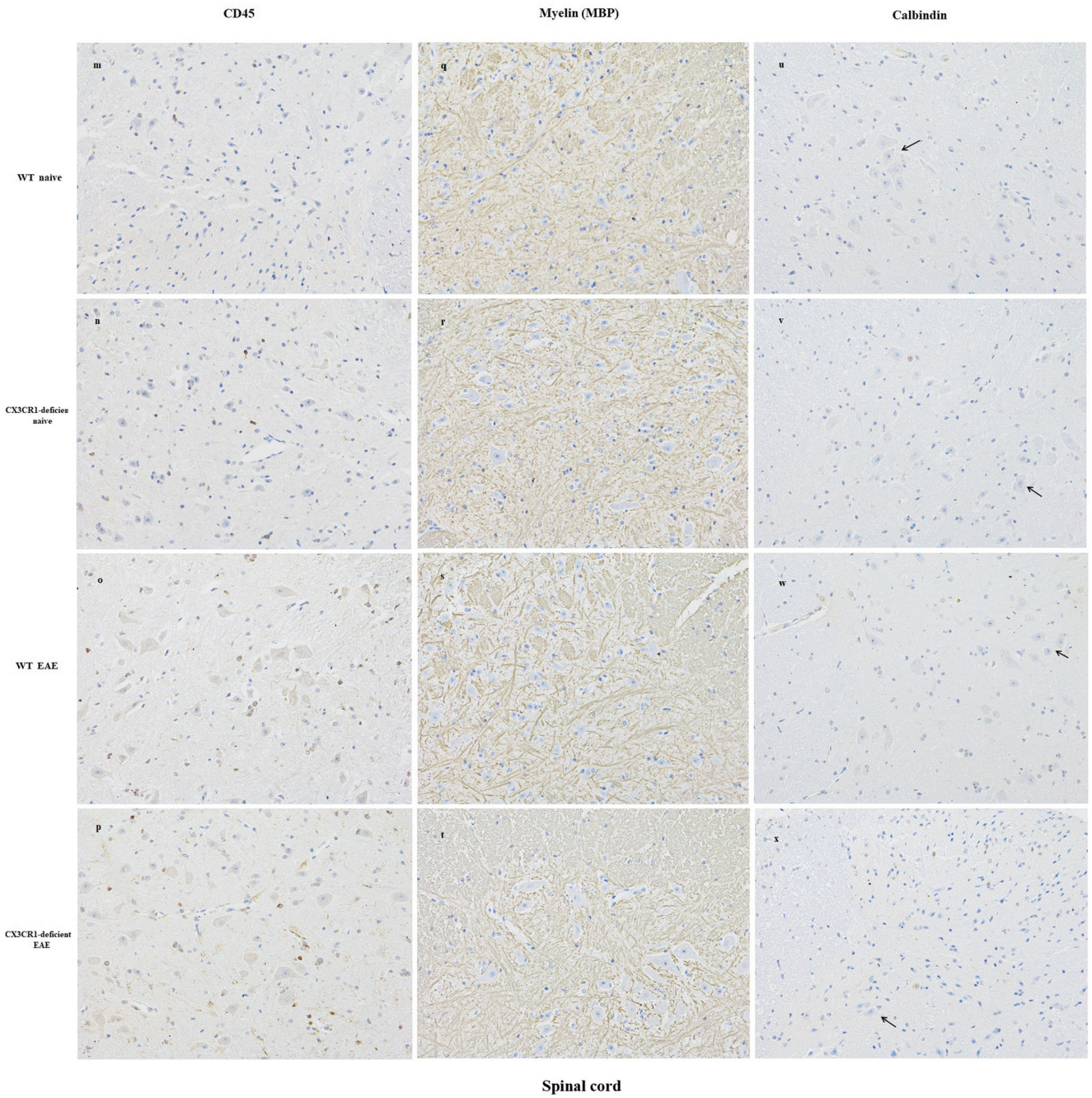

Fig. 3 continued.

in WT EAE mice was less darker than in WT naive and CX3CR1$^{GFP/GFP}$ naive mice. In CX3CR1$^{GFP/GFP}$ EAE mice, the intensity of the myelin staining decreased more remarkably. In addition, in WT EAE mice, calbindin-positive neurons were visualized along the granular cell layer in the cerebellar region, just as WT naive and CX3CR1$^{GFP/GFP}$ naive mice. But in CX3CR1$^{GFP/GFP}$ EAE mice, calbindin-positive neurons were destroyed with the disruption of the granular cell layer. Quantitative analysis revealed that IOD of myelin immunoreactivity in CX3CR1-deficient EAE mice was reduced, compared with WT EAE, WT naive, and CX3CR1-deficient naive mice (5919.1 ± 176.96 vs 15,361.8 ± 1505.51, P = 0.004, Z = − 2.882; 5919.1 ± 176.96 vs 44,674.0 ± 2015.26, P = 0.004, Z = − 2.882; 5919.1 ± 176.96 vs 43,479.0 ± 1881.21, P = 0.004, Z = − 2.882). IOD of myelin immunoreactivity in WT EAE mice was lower than in WT naive mice (15,361.8 ± 1505.51 vs 44,674.0 ± 2015.26, P = 0.004, Z = − 2.882). But there were no significant differences of myelin immunoreactivity IOD between WT naive and CX3CR1-deficient naive mice (44,674.0 ± 2015.26 vs 43,479.0 ±

1881.21, $P = 0.522$, $Z = -0.641$). The results indicated that in CX3CR1-deficient EAE mice, CNS inflammation controlled by infiltrating myeloid cells was associated with enhanced CNS demyelination and neuron damage.

Elevated expression of MHC-II on CD11c$^+$ dendritic cells in the brain of CX3CR1-deficient EAE mice

The expressions of MHC-II on brain myeloid cells were analyzed by flow cytometry. We found that surface expression of MHC-II on brain CD45$^+$CD115$^+$Ly6C$^-$CD11c$^+$ cells of CX3CR1-deficient EAE mice was upregulated when compared with WT EAE mice (mean fluorescence intensity (MFI), 2442.0 ± 163.73 vs 1745.4 ± 25.67, $P = 0.003$, $F = 17.677$; percentage of MHC-II-FITC high subset, 18.7 ± 3.55% vs 6.6 ± 0.36%, $P = 0.008$, $Z = -2.643$) (Fig. 4). Besides, in both CX3CR1-deficient and WT EAE mice, MHC-II expressions on brain CD45$^+$CD11c$^+$ cells were higher than that on CD45$^+$CD11c$^-$ cells (CX3CR1-deficient EAE mice, MFI 2226.0 ± 105.48 vs 1126.8 ± 90.48, $P = 0.000$, $F = 62.561$; WT EAE mice, MFI 1710.0 ± 49.09 vs 1235.6 ± 67.94, $P = 0.000$, $F = 32.033$).

Increased expressions of MHC-II in the affected brain of CX3CR1-deficient EAE mice

The expressions of MHC-II in the brain of WT and CX3CR1-deficient EAE mice were further detected by quantitative real-time RT-PCR and western blotting. It was shown that mRNA expressions of MHC-II in the affected brain of CX3CR1-deficient EAE mice were elevated, compared with CX3CR1-deficient naive, WT naive, and WT EAE mice (17.86 ± 0.199 vs 0.70 ± 0.104, $P = 0.000$; 17.86 ± 0.199 vs 0.67 ± 0.149, $P = 0.000$; 17.86 ± 0.199 vs 7.01 ± 0.154, $P = 0.000$). The mRNA expressions of MHC-II in the affected brain of WT EAE mice were higher than that of WT naive

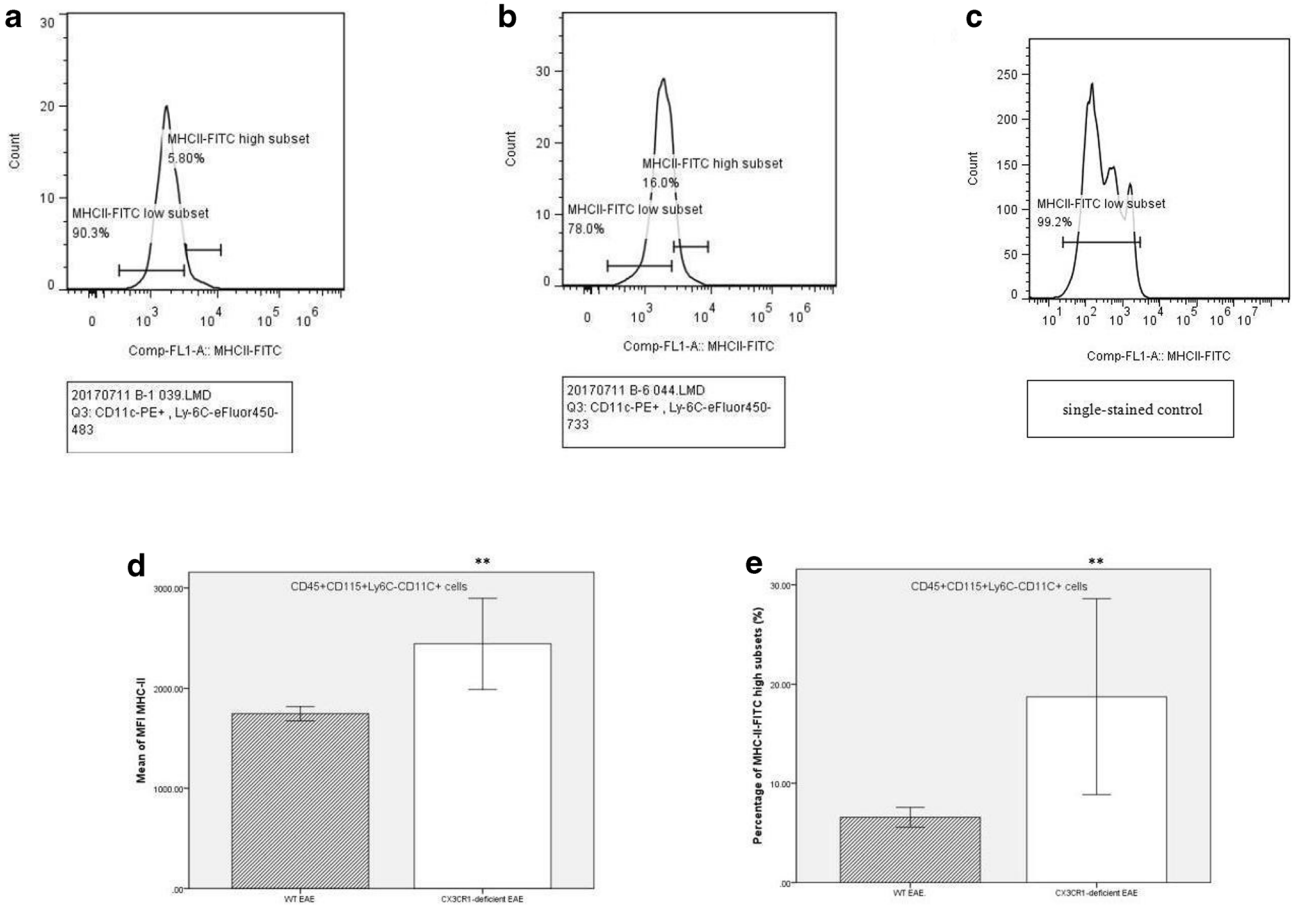

Fig. 4 Effects of CX3CR1 on MHC-II of antigen-presenting cells. The expressions of MHC-II on brain myeloid cells from CX3CR1$^{GFP/GFP}$ and WT EAE mice at the peak of disease were analyzed by flow cytometry. Representative FACS profiles of percentage of MHC-II-FITC high subset on brain CD45$^+$CD115$^+$Ly6C$^-$CD11c$^+$ cells of WT EAE mice (**a**) and CX3CR1-deficient EAE mice (**b**), with single-stained controls for fluorescence compensation (**c**). Mean fluorescence intensity (MFI) of MHC-II (**d**) and percentage of MHC-II-FITC high subset (**e**) on brain CD45$^+$CD115$^+$Ly6C$^-$CD11c$^+$ cells of CX3CR1-deficient EAE mice were elevated when compared with WT EAE mice. Data were presented as mean ± SEM of five independent experiments. $^{**}P < 0.01$ by one-way ANOVA and Mann-Whitney *U* test, respectively (versus WT EAE mice)

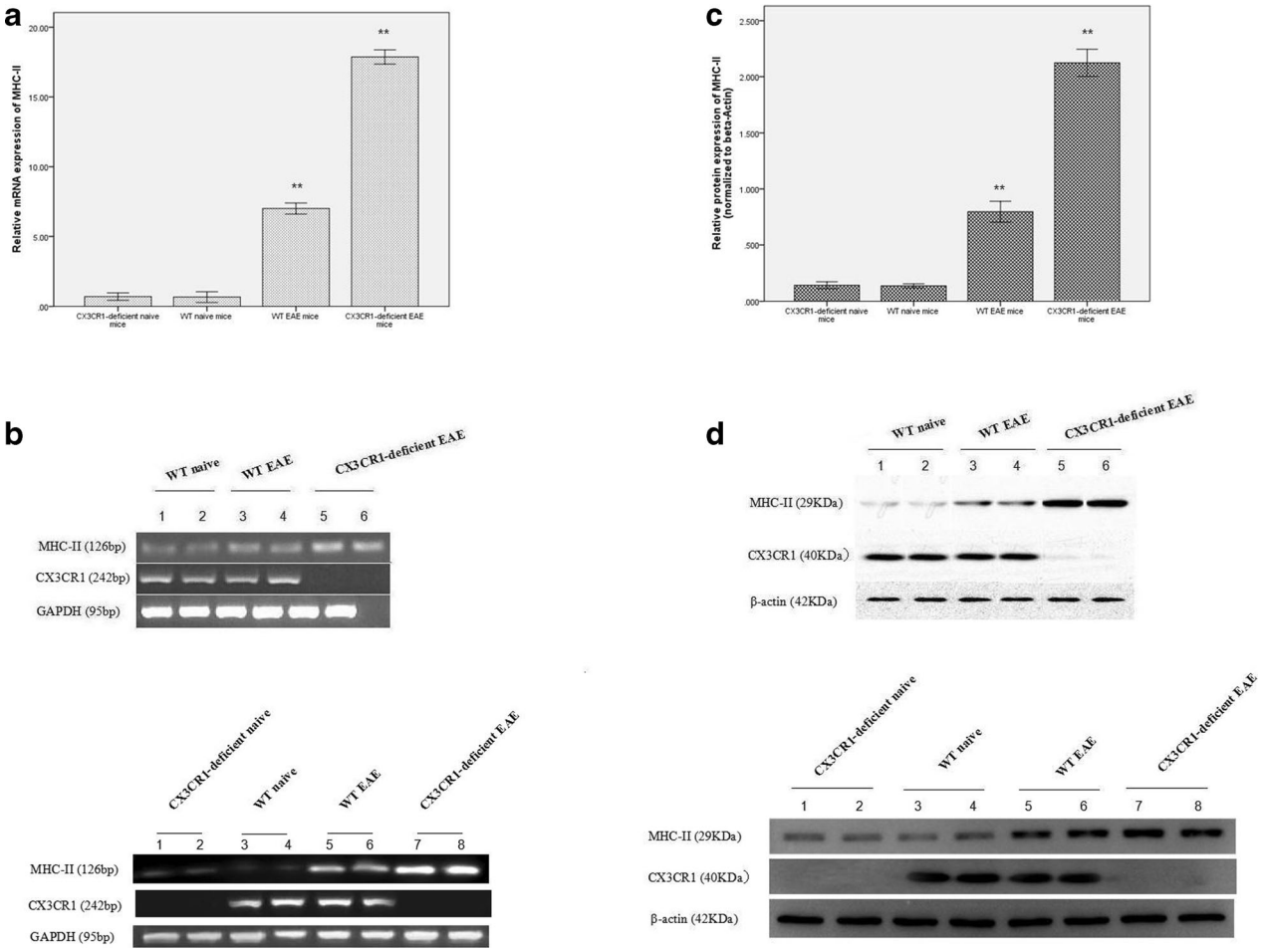

Fig. 5 Increased expressions of MHC-II in the affected brain of CX3CR1-deficient EAE mice. The mRNA and protein expressions of MHC-II in the brain were analyzed by quantitative real-time RT-PCR and western blotting, respectively. a Compared with CX3CR1-deficient naive, wild-type (WT) naive, and WT EAE mice, MHC-II mRNA expressions in the affected brain of CX3CR1-deficient EAE mice were elevated. Data were presented as mean ± SEM of six independent experiments. $^{**}P < 0.01$ by one-way ANOVA and LSD for pairwise comparisons (versus CX3CR1-deficient naive, WT naive, and WT EAE mice). **b** Representative agarose electropherogram of MHC-II and CX3CR1 in RT-PCR, using GAPDH as internal control. In the upper panel, lands 1, 2 represented WT naive mice; lands 3, 4 represented WT EAE mice; and lands 5, 6 represented CX3CR1-deficient EAE mice. In the lower panel, lands 1, 2 represented CX3CR1-deficient naive mice; lands 3, 4 represented WT naive mice; lands 5, 6 represented WT EAE mice; and lands 7, 8 represented CX3CR1-deficient EAE mice. **c** Compared with CX3CR1-deficient naive, WT naive, and WT EAE mice, MHC-II protein expressions in the affected brain of CX3CR1-deficient EAE mice were also elevated. Data were presented as mean ± SEM of three independent experiments. $^{**}P < 0.01$ by one-way ANOVA and LSD for pairwise comparisons (versus CX3CR1-deficient naive, WT naive, and WT EAE mice). **d** Representative western blotting of MHC-II and CX3CR1 proteins, using β-actin as internal control. In the upper panel, lands 1, 2 represented WT naive mice; lands 3, 4 represented WT EAE mice; and lands 5, 6 represented CX3CR1-deficient EAE mice. In the lower panel, lands 1, 2 represented CX3CR1-deficient naive mice; lands 3, 4 represented WT naive mice; lands 5, 6 represented WT EAE mice; and lands 7, 8 represented CX3CR1-deficient EAE mice

mice (7.01 ± 0.154 vs 0.67 ± 0.149, $P = 0.000$). There were no significant differences in MHC-II mRNA expressions between WT naive and CX3CR1-deficient naive mice (0.67 ± 0.149 vs 0.70 ± 0.104, $P = 0.881$) (Fig. 5a, b).

As presented in Fig. 5c and d, the protein expressions of MHC-II in the affected brain of CX3CR1-deficient EAE mice were also increased, compared with CX3CR1-deficient naive, WT naive, and WT EAE mice (relative grayscale, 2.12 ± 0.028 vs 0.14 ± 0.007, $P = 0.000$; 2.12 ± 0.028 vs 0.13 ± 0.004, $P = 0.000$; 2.12 ± 0.028 vs 0.80 ± 0.022, $P = 0.000$). The protein expressions of MHC-II in the affected brain of WT EAE mice were higher than that of WT naive mice (relative grayscale, 0.80 ± 0.022 vs 0.13 ± 0.004, $P = 0.000$). There were no significant differences in MHC-II protein expressions between WT naive and CX3CR1-deficient naive mice (relative grayscale, 0.13 ± 0.004 vs 0.14 ± 0.007, $P = 0.619$).

Increased expressions of CIITA and IRF-1 in the affected brain of CX3CR1-deficient EAE mice

The expressions of CIITA and IRF-1, two major MHC-II gene regulators, in the brain were analyzed by quantitative real-time

RT-PCR and western blotting, respectively. The data showed that the mRNA expressions of CIITA and IRF-1 in the affected brain of CX3CR1-deficient EAE mice were elevated, compared with CX3CR1-deficient naive, WT naive, and WT EAE mice (CIITA, 7.74 ± 1.237 vs 0.67 ± 0.111, $P = 0.004$, $Z = -2.882$; 7.74 ± 1.237 vs 0.63 ± 0.170, $P = 0.004$, $Z = -2.903$; 7.74 ± 1.237 vs 2.80 ± 0.361, $P = 0.004$, $Z = -2.882$. IRF-1, 15.88 ± 0.920 vs 0.75 ± 0.087, $P = 0.004$, $Z = -2.882$; 15.88 ± 0.920 vs 0.66 ± 0.153, $P = 0.004$, $Z = -2.903$; 15.88 ± 0.920 vs 3.98 ± 0.870, $P = 0.004$, $Z = -2.882$). The mRNA

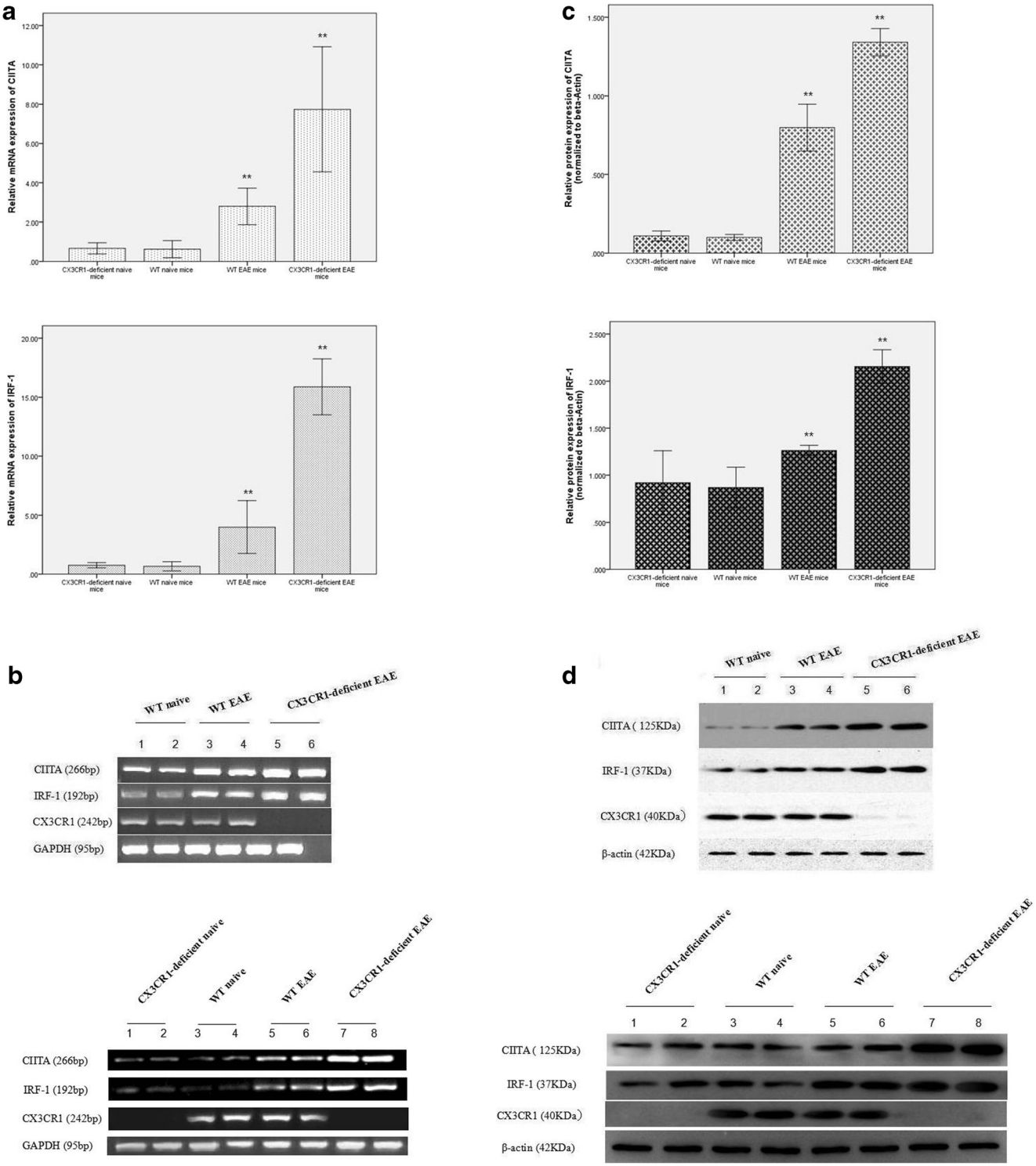

◀ **Fig. 6** Increased expressions of CIITA and IRF-1 in the affected brain of CX3CR1-deficient EAE mice. The mRNA and protein expressions of CIITA and IRF-1 in the brain were analyzed by quantitative real-time RT-PCR and western blotting, respectively. **a** Compared with CX3CR1-deficient naive, wild-type (WT) naive, and WT EAE mice, CIITA and IRF-1 mRNA expressions in the affected brain of CX3CR1-deficient EAE mice were elevated. Data were presented as mean ± SEM of six independent experiments. $^{**}P < 0.01$ by non-parametric Mann-Whitney *U* test (versus CX3CR1-deficient naive, WT naive, and WT EAE mice). **b** Representative agarose electropherogram of CIITA, IRF-1, and CX3CR1 in RT-PCR, using GAPDH as internal control. In the upper panel, lands 1, 2 represented WT naive mice; lands 3, 4 represented WT EAE mice; and lands 5, 6 represented CX3CR1-deficient EAE mice. In the lower panel, lands 1, 2 represented CX3CR1-deficient naive mice; lands 3, 4 represented WT naive mice; lands 5, 6 represented WT EAE mice; and lands 7, 8 represented CX3CR1-deficient EAE mice. **c** Compared with CX3CR1-deficient naive, WT naive, and WT EAE mice, CIITA and IRF-1 protein expressions in the affected brain of CX3CR1-deficient EAE mice were increased. Data were presented as mean ± SEM of three independent experiments. $^{**}P < 0.01$ by one-way ANOVA and LSD for pairwise comparisons (versus CX3CR1-deficient naive, WT naive, and WT EAE mice). **d** Representative western blotting of CIITA, IRF-1, and CX3CR1 proteins, using β-actin as internal control. In the upper panel, lands 1, 2 represented WT naive mice; lands 3, 4 represented WT EAE mice; and lands 5, 6 represented CX3CR1-deficient EAE mice. In the lower panel, lands 1, 2 represented CX3CR1-deficient naive mice; lands 3, 4 represented WT naive mice; lands 5, 6 represented WT EAE mice; and lands 7, 8 represented CX3CR1-deficient EAE mice

expressions of CIITA and IRF-1 in the affected brain of WT EAE mice were higher than that of WT naive mice (CIITA, 2.80 ± 0.361 vs 0.63 ± 0.170, $P = 0.004$, $Z = -2.903$; IRF-1, 3.98 ± 0.870 vs 0.66 ± 0.153, $P = 0.004$, $Z = -2.903$). There were no significant differences of CIITA and IRF-1 mRNA expressions between WT naive and CX3CR1-deficient naive mice (CIITA, 0.63 ± 0.170 vs 0.67 ± 0.111, $P = 0.935$, $Z = -0.082$; IRF-1, 0.66 ± 0.153 vs 0.75 ± 0.087, $P = 0.807$, $Z = -0.245$) (Fig. 6a, b).

As presented in Fig. 6c and d, the protein expressions of CIITA and IRF-1in the affected brain of CX3CR1-deficient EAE mice were also increased, compared with CX3CR1-deficient naive, WT naive, and WT EAE mice (relative grayscale: CIITA, 1.34 ± 0.020 vs 0.11 ± 0.007, $P = 0.000$; 1.34 ± 0.020 vs 0.10 ± 0.004, $P = 0.000$; 1.34 ± 0.020 vs 0.80 ± 0.035, $P = 0.000$; IRF-1: 2.15 ± 0.042 vs 0.92 ± 0.079, $P = 0.000$; 2.15 ± 0.042 vs 0.87 ± 0.050, $P = 0.000$; 2.15 ± 0.042 vs 1.26 ± 0.013, $P = 0.000$). The protein expressions of CIITA and IRF-1in the affected brain of WT EAE mice were higher than that of WT naive mice (relative grayscale: CIITA, 0.80 ± 0.035 vs 0.10 ± 0.004, $P = 0.000$; IRF-1, 1.26 ± 0.013 vs 0.87 ± 0.050, $P = 0.001$). There were no significant differences of CIITA and IRF-1 protein expressions between WT naive and CX3CR1-deficient naive mice (relative grayscale: CIITA, 0.10 ± 0.004 vs 0.11 ± 0.007, $P = 0.745$; IRF-1, 0.87 ± 0.050 vs 0.92 ± 0.079, $P = 0.507$).

Correlation between MHC-II expressions and CIITA and IRF-1

Both mRNA and protein expressions of MHC-II in the brain positively correlated with CIITA and IRF-1, respectively (MHC-II and CIITA: mRNA $r = 0.903$, $P = 0.000$; protein $r = 0.970$, $P = 0.000$; MHC-II and IRF-1: mRNA $r = 0.959$, $P = 0.000$; protein $r = 0.988$, $P = 0.000$).

Discussion

CX3CR1, the unique receptor of CX3CL1, is expressed by microglia in the CNS. Besides controlling leukocyte migration, recent evidence from animal experiments and genetic studies has implicated a neuroprotective role of CX3CR1 in MS. In this experiment, CX3CR1-deficient mice were generated according to the methods described by Jung S [14] and genotyped by RT-PCR analysis. It was shown that in $CX3CR1^{+/GFP}$ mice, chimeric transcripts (both WT and mutant CX3CR1 transcripts) were presented, but in $CX3CR1^{GFP/GFP}$ mice, only mutant CX3CR1 transcripts were presented. Using this animal model, we identified that CX3CR1-deficient mice with EAE exhibited more severe disease severity defined by earlier onset and higher maximum EAE scores. In addition, enhanced CNS pathology including exacerbated inflammatory infiltration, demyelination, and Purkinje cell damage was also observed in CX3CR1-deficient EAE mice. Our findings supported a beneficial role of CX3CR1 in a chronic EAE model for MS, consistent with former literature [10, 11]. However, Ridderstad Wollberg et al. reported that pharmacological inhibition of CX3CR1 with selective CX3CR1 inhibitor AZD8797 reduced inflammation and degeneration in the CNS in a disease model for MS [16]. Their results seemed to be in contrast with our study. The basis for this is unclear. In view of different EAE models used, potential differences between $MOG_{35–55}$-induced EAE in C57BL/6 mice and $MOG_{1–125}$-induced EAE in DA rats may contribute to the divergent results. Besides, different study methods, gene deletion or blocking CX3CR1 with AZD8797, may also cause complex impacts.

So far, the mechanism for the protective effects of CX3CR1 in MS remains unclear. Monocytes, critical mediators of innate and adaptive immunity [17], play an important role in MS and EAE. Based on the expressions of CX3CR1 and chemokine receptor 2 (CCR2), blood monocytes can be divided into two subsets: "inflammatory" and "patrolling" monocytes, distinguished as $Ly6C^{+}CCR2^{hi}CX3CR1^{lo}$ and $Ly6C^{-}CCR2^{lo}CX3CR1^{hi}$ in mice, respectively. "Inflammatory" monocytes are actively recruited to inflamed tissues and undergo activation, whereas "patrolling" monocytes patrol the vascular endothelial lumen and involve in surveillance [18–20]. Similar to the blood monocyte subsets,

resident microglia and infiltrating monocytes in the EAE brain can also be defined by CX3CR1 expressions [19], recognized as $CCR2^{lo}CX3CR1^{hi}$ and $CCR2^{hi}CX3CR1^{lo}$ separately. In a model of excitotoxicity, it was demonstrated that patrolling monocytes played a critical role in CX3CR1-mediated neuroprotection [21]. Therefore, we intended to investigate the role of CX3CR1 on the infiltration of myeloid cells to the CNS in EAE. As a result, we observed an accumulation of $CD45^{+}CD115^{+}Ly6C^{-}CD11c^{+}$ dendritic cells in the affected EAE brain of CX3CR1-deficient mice, as well as enhanced inflammation, demyelination, and Purkinje cell damage in the CNS. This is in accord with previous study [10], implicating an important role of CX3CR1 for antigen-presenting cells (APCs) in MS, which might be involved in anti-myelin T cell stimulation.

However, whether CX3CR1 participates in modulation of antigen presentation by APC and what the possible mechanism is remain unclear. MHC-II, a class of molecules constitutively expressed on APCs, is known to be essential in initiating immune responses. Only when the specific T cell receptor on the activated anti-myelin T cells that entered the CNS recognizes its myelin antigen presented on the surface of APCs combined with MHC-II can the anti-myelin T cells be reactivated. Thus, in this study, brain cells isolated at the peak of EAE were analyzed for MHC-II by flow cytometry. The data showed that the expressions of MHC-II on brain $CD45^{+}CD115^{+}Ly6C^{-}CD11c^{+}$ dendritic cells of CX3CR1-deficient EAE mice were elevated, compared with wild-typed EAE mice. In addition, the protein and mRNA expressions of MHC-II in the brain of CX3CR1-deficient EAE mice were also upregulated. These supported that CX3CR1 was associated with MHC-II expression, which was involved in the modulation of antigen presentation by APC.

We sought to further investigate the mechanism linking CX3CR1 to MHC-II gene regulation. It is known that several transcription factors including CIITA, STAT, and IRF-1 are involved in the regulation of MHC-II gene. CIITA, a non-DNA-binding protein, acts as a key positive regulator of MHC-II gene transcription, through binding with the upstream promoter elements that are bound by CREB (cyclic AMP response element-binding protein), RFX (regulatory factor X), and NF-γ (nuclear factor γ) [22, 23]. STAT and IRF-1, two transcription factors that bind to the CIITA promoter IV, regulate the expression of CIITA gene [24–26]. In the current study, the protein and mRNA expressions of CIITA and IRF-1 in the affected brain at peak of EAE were assessed by western-blot and real-time RT-PCR. The data revealed that both the protein and mRNA expressions of CIITA and IRF-1 in the brain of CX3CR1-deficient EAE mice were elevated, which correlated with the increased MHC-II expressions. This implicated that CIITA and IRF-1 might be the potential targets of CX3CR1, involved in regulation of MHC-II expressions and modulation of antigen presentation in APC.

Conclusions

In summary, our data supported a beneficial role of CX3CR1 in a chronic EAE model for MS, involved in modulation of infiltrating myeloid cells ($CD45^{+}CD115^{+}Ly6C^{-}CD11c^{+}$ subset) to the CNS. Besides, CX3CR1 was associated with MHC-II expressions on APCs, implicated in modulation of antigen presentation. Our findings also indicated that the mechanism linking CX3CR1-CX3CL1 interaction to modulation of antigen presentation was probably through regulation on the MHC-II regulators CIITA and IRF-1. This advances our understanding and provides new insights into the mechanism for neuroprotective role of CX3CR1 in the EAE model for MS.

Funding information This work was supported by the Natural Science Foundation of Guangdong Province, China (Grant No: 2014A030313028), and Science and Technology Planning Project of Zhuhai city, China (Grant No: 2015A1011).

Compliance with ethical standards

Conflict of interest The authors declare that they have no conflict of interest.

References

1. Serbina NV, Pamer EG (2006) Monocyte emigration from bone marrow during bacterial infection requires signals mediated by chemokine receptor CCR2. Nat Immunol 7:311–317
2. Auffray C, Sieweke M, Geissmann F (2009) Blood monocytes: development, heterogeneity, and relationship with dendritic cells. Annu Rev Immunol 27:669–692
3. Cardona AE, Pioro EP, Sasse ME, Kostenko V, Cardona SM, Dijkstra IM, Huang D, Kidd G, Dombrowski S, Dutta R, Lee JC, Cook DN, Jung S, Lira SA, Littman DR, Ransohoff RM (2006) Control of microglial neurotoxicity by the fractalkine receptor. Nat Neurosci 9:917–924
4. Hatori K, Nagai A, Heisel R, Ryu JK, Kim SU (2002) Fractalkine and fractalkine receptors in human neurons and glial cells. J Neurosci Res 69:418–426
5. Tuo J, Smith BC, Bojanowski CM, Meleth AD, Gery I, Csaky KG, Chew EY, Chan CC (2004) The involvement of sequence variation and expression of CX3CR1 in the pathogenesis of age-related macular degeneration. FASEB J 18:1297–1299
6. Chan CC, Tuo J, Bojanowski CM, Csaky KG, Green WR (2005) Detection of CX3CR1 single nucleotide polymorphism and expression on archived eyes with age-related macular degeneration. Histol Histopathol 20:857–863
7. Meucci O, Fatatis A, Simen AA, Miller RJ (2000) Expression of CX3CR1 chemokine receptors on neurons and their role in neuronal survival. Proc Natl Acad Sci U S A 97:8075–8080
8. Lauro C, Di Angelantonio S, Cipriani R, Sobrero F, Antonilli L, Brusadin V, Ragozzino D, Limatola C (2008) Activity of adenosine receptors type 1 is required for CX3CL1-mediated neuroprotection and neuromodulation in hippocampal neurons. J Immunol 180:7590–7596

9. Lauro C, Cipriani R, Catalano M, Trettel F, Chece G, Brusadin V, Antonilli L, van Rooijen N, Eusebi F, Fredholm BB, Limatola C (2010) Adenosine A1 receptors and microglial cells mediate CX3CL1-induced protection of hippocampal neurons against Glu-induced death. Neuropsychopharmacology 35:1550–1559
10. Garcia JA, Pino PA, Mizutani M, Cardona SM, Charo IF, Ransohoff RM, Forsthuber TG, Cardona AE (2013) Regulation of adaptive immunity by the fractalkine receptor during autoimmune inflammation. J Immunol 191:1063–1072
11. Stojković L, Djurić T, Stanković A, Dinčić E, Stančić O, Veljković N, Alavantić D, Zivković M (2012) The association of V249I and T280M fractalkine receptor haplotypes with disease course of multiple sclerosis. J Neuroimmunol 245:87–92
12. Huang D, Shi FD, Jung S, Pien GC, Wang J, Salazar-Mather TP, He TT, Weaver JT, Ljunggren HG, Biron CA, Littman DR, Ransohoff RM (2006) The neuronal chemokine CX3CL1/fractalkine selectively recruits NK cells that modify experimental autoimmune encephalomyelitis within the central nervous system. FASEB J 20: 896–905
13. De Keyser J, Laureys G, Demol F, Wilczak N, Mostert J, Clinckers R (2010) Astrocytes as potential targets to suppress inflammatory demyelinating lesions in multiple sclerosis. Neurochem Int 57:446–450
14. Jung S, Aliberti J, Graemmel P, Sunshine MJ, Kreutzberg GW, Sher A, Littman DR (2000) Analysis of fractalkine receptor CX(3)CR1 function by targeted deletion and green fluorescent protein reporter gene insertion. Mol Cell Biol 20:4106–4114
15. Pluchino S, Quattrini A, Brambilla E, Gritti A, Salani G, Dina G, Galli R, Del Carro U, Amadio S, Bergami A, Furlan R, Comi G, Vescovi AL, Martino G (2003) Injection of adult neurospheres induces recovery in a chronic model of multiple sclerosis. Nature 422: 688–694
16. Ridderstad Wollberg A, Ericsson-Dahlstrand A, Juréus A, Ekerot P, Simon S, Nilsson M, Wiklund SJ, Berg AL, Ferm M, Sunnemark D, Johansson R (2014) Pharmacological inhibition of the chemokine receptor CX3CR1 attenuates disease in a chronic-relapsing rat model for multiple sclerosis. Proc Natl Acad Sci U S A 111:5409–5414
17. Geissmann F, Manz MG, Jung S, Sieweke MH, Merad M, Ley K (2010) Development of monocytes, macrophages, and dendritic cells. Science 327:656–661
18. Geissmann F, Jung S, Littman DR (2003) Blood monocytes consist of two principal subsets with distinct migratory properties. Immunity 19:71–82
19. Saederup N, Cardona AE, Croft K, Mizutani M, Cotleur AC, Tsou CL, Ransohoff RM, Charo IF (2010) Selective chemokine receptor usage by central nervous system myeloid cells in CCR2-red fluorescent protein knock-in mice. PLoS One 5:e13693
20. Platt AM, Mowat AM (2008) Mucosal macrophages and the regulation of immune responses in the intestine. Immunol Lett 119:22–31
21. Bellavance MA, Gosselin D, Yong VW, Stys PK, Rivest S (2015) Patrolling monocytes play a critical role in CX3CR1-mediated neuroprotection during excitotoxicity. Brain Struct Funct 220:1759–1776
22. Harton JA, Ting JP (2000) Class II transactivator: mastering the art of major histocompatibility complex expression. Mol Cell Biol 20: 6185–6194
23. Moreno CS, Beresford GW, Louis-Plence P, Morris AC, Boss JM (1999) CREB regulates MHC class II expression in a CIITA-dependent manner. Immunity 10:143–151
24. Nikodemova M, Watters JJ, Jackson SJ, Yang SK, Duncan ID (2007) Minocycline down-regulates MHC II expression in microglia and macrophages through inhibition of IRF-1 and protein kinase C (PKC) alpha/beta II. J Biol Chem 282:15208–15216
25. Barbaro Ade L, Tosi G, Frumento G, Bruschi E, D'Agostino A, Valle MT, Manca F, Accolla RS (2002) Block of Stat-1 activation in macrophages phagocytosing bacteria causes reduced transcription of CIITA and consequent impaired antigen presentation. Eur J Immunol 32:1309–1318
26. Stickel N, Hanke K, Marschner D, Prinz G, Köhler M, Melchinger W, Pfeifer D, Schmitt-Graeff A, Brummer T, Heine A, Brossart P, Wolf D, von Bubnoff N, Finke J, Duyster J, Ferrara J, Salzer U, Zeiser R (2017) MicroRNA-146a reduces MHC-II expression via targeting JAK/STAT signaling in dendritic cells after stem cell transplantation. Leukemia 31:2732–2741